CrossMark

ORIGINAL ARTICLE

Characterization of active and closed landfill sites using 2D resistivity/IP imaging: case studies in Penang, Malaysia

Abdullahi Abdulrahman[1,4] · Mohd Nawawi[1] · Rosli Saad[1] · Asad Siraj Abu-Rizaiza[2] · Mohd Suffian Yusoff[3] · Amin Esmail Khalil[1,5] · Kehinde Saheed Ishola[1,6]

Abstract An interpretation approach for analysis of electrical resistivity and chargeability inverse models generated at two upgraded semi-aerobic landfill sites was developed. The inverse models produced from a 2D inversion program (RES2DINV) were used to set up a grid of electrical resistivity and chargeability imaging at the landfill sites. The investigations confirmed a high chargeability unit (>70 ms) depicting waste deposits and a saturated clayey layer, while the leachate plume showed low resistivity ($<10\ \Omega$m) and weak chargeability zone (<20 ms). Moreover, the IP responses of a diffused leachate plume downstream of a separate semi-aerobic landfill site in a similar geological setting were evaluated, obtaining an analogous result. The ion-dominated plume that exhibited a weak chargeability promoted membrane polarization rather than electrode polarization in its IP responses. However, the high concentration of ions in the diffused leachate restrained the ionic polarization, diminishing the IP effects in host sediments. The interpretation of the resistivity and chargeability profiles at the characterization sites allowed delineating the different zones of the subsurface strata. In particular, comparison of the leachate zones at the two locations revealed that the active landfill with a lesser proportion of waste deposits contained a greater accumulation of leachate than the closed site. The results in this study support the effectiveness of contaminant plume monitoring through the joint application of resistivity and IP methods. These non-invasive, rapid and cost-effective, geophysical techniques could lead to a promising reconnaissance tool for remediation or reclamation of solid waste disposal sites.

Keywords Resistivity · IP · Chargeability · Leachate · Waste deposit · Landfill

Introduction

Landfilling is the most common solid waste management system worldwide (Morris and Barlaz 2011). The growing global population has increased the demand for proper supervision of landfill sites, especially in view of the sprawl of developments over such facilities. However, most old and abandoned landfills in developing countries lack containment objectives (Inanc et al. 2004; Singh et al. 2011). Leachate from these unregulated discharges poses a health hazard to the nearby community and has adverse effects on local ecosystems (Aluko and Sridhar 2005). Accordingly, full characterization and monitoring of these landfills is essential to risk assessment and management of the overall environment.

Non-invasive and rapid surface geophysical surveys serve as complementary tools to monitoring wells for

✉ Abdullahi Abdulrahman
aa11_phy077@student.usm.my;
aabdulrahman@atbu.edu.ng

1 Geophysics Unit, School of Physics, Universiti Sains Malaysia, 11800 Penang, Malaysia

2 Environmental Science Department, King Abdulaziz University, Jeddah, Saudi Arabia

3 School of Civil Engineering, Universiti Sains Malaysia, 14300 Penang, Malaysia

4 Department of Physics, Abubakar Tafawa Balewa University, Bauchi, Nigeria

5 Geology Department, Faculty of Science, Helwan University, Helwan, Egypt

6 Department of Geosciences, University of Lagos, Akoka, Nigeria

evaluation of landfill sites and their surrounding environments. A great deal of the literature regarding the application of geoelectrical methods for monitoring or characterization of dumpsites is available (Kelly 1976; Frohlich et al. 1994; Meju 2000; Yoon et al. 2003; Mota et al. 2004; Naudet et al. 2004; Chambers et al. 2006; Soupios et al. 2007; Abdulrahman et al. 2013). Leachate plumes from landfill sites contain high levels of ions that reduce the resistivity of contaminated areas, which distinguishes these zones from surrounding areas and makes monitoring using electrical resistivity probes plausible (Bernstone and Dahlin 1999).

If there is a small contrast in resistivity between the leachate plume and a background with low resistivity, the resistivity approach will not be adequate to map the leachate plume (Carlson et al. 2001). For example, a low resistivity anomaly can be generated by an increase in ion content in formations with a higher saturation or a higher clay content in areas of sandy sediment. However, such areas could be distinguished if the chargeability of the sediments were also known (Dahlin et al. 2002). Saline water that has high ionic conductivity shows poor chargeability in contrast with clayey layers that generate high IP responses (Sharma 1997; Martinho and Almeida 2006; Gazoty et al. 2012a). The integration of electrical resistivity and IP investigative techniques can help to distinguish between clay and sand bearing salt water, which both show low resistivity.

Gazoty et al. (2012a) reported that ambiguities in electrical resistivity surveys are generated when the water table is within the waste deposits. Indeed, the dependence of electrical responses on pore fluid introduces large uncertainties in landfill mapping. However, the combination of electrical resistivity and IP removes some of the doubts arising from the separate utilization of these techniques. While the resistivity method responds to saturation, IP depends on lithology and chargeable units associated with landfills (Legaz et al. 2010). Several studies have shown the advantages of integrating the two methods for characterization of solid waste disposal sites (Abu-Zeid et al. 2004; Aristodemou and Thomas-Betts 2000; Dahlin et al. 2010; Ustra et al. 2012).

Interpretation of electrical resistivity inverse models at landfill sites is less controversial than analysis of chargeability models. Soil resistivity mainly depends on sediment porosity, water content, and water resistivity (Archie 1942). Low resistivity values are typical of seawater, brackish water, leachate, and clay. Intermediate resistivity values are associated with fresh water, wet sand, sandstone, and limestone formations, while high resistivity corresponds to dry sand or granite bedrock (Guérin et al. 2004). Despite the certainty in distinguishing clay from other unconsolidated sediments because of its high IP response

(Iliceto et al. 1982; Slater and Lesmes 2002; Turesson and Lind 2005; Slater et al. 2006; Breede and Kemna 2012; Gazoty et al. 2012b), the chargeability status of the disseminated contaminant plume requires comprehensive evaluation. Notwithstanding, the metallic content of waste generates high chargeability, which makes demarcation of solid waste boundaries at landfill sites using IP surveys attractive (Aristodemou and Thomas-Betts 2000; Wynn and Grosz 2000; Ustra et al. 2012).

The correct assessment of the IP response produced by diffused leachate plumes is essential to adequate characterization of contaminated sites. However, this topic is still under discussion. Some authors delineate dispersed waste free plumes as high chargeability zones (Aristodemou and Thomas-Betts 2000; Abu-Zeid et al. 2004; Martinho and Almeida 2006), whereas Gallas et al. (2011) postulated that disseminated plumes exhibit low chargeability in host sediments, despite the high ionic content. Dahlin et al. (2010) superimposed resistivity and chargeability models at landfill sites, and this integration reflected the mixture of leachate and waste as a region of high chargeability combined with low resistivity. The resistivity models demarcated the leachate zones while chargeability models delineated the waste areas. These results suggest that the leachate plume is more susceptible to a resistivity evaluation rather than an IP assessment, since the contaminant regions exhibited insignificant IP responses. Their findings also showed that solid waste and uncontaminated saturated soil have similar resistivity responses, and therefore cannot be distinguished using resistivity models. However, the chargeability evaluation indicated the waste had a high IP response and the saturated soil (not clay) had weak IP signals.

The objective of the present study was to provide a procedure for detailed characterization of the subsurface of landfill sites using electrical resistivity and time domain IP imaging techniques. The challenges associated with the chargeability of the leachate plume were also addressed, and the possibility of delineation of contaminated sites with minimal ground truthing was assessed. A separate semi-aerobic disposal site with nearby boreholes located downstream was used to evaluate the chargeability responses of the diffused leachate plume discharged from aeration ponds. The grid acquisition of IP and electrical resistivity data at the two selected landfills was employed to demarcate zones containing buried waste, regions containing only leachate, and uncontaminated subsoil volumes.

Description of landfill sites

This study investigated two upgraded semi-aerobic landfills, the closed Ampang Jajar Landfill (AJL) and the active Pulau Burung landfill (PBL), which are located in Seberang

Perai, the mainland section of the state of Penang, Malaysia. The Penang Mainland is within lowlands and the coastal area of Peninsular Malaysia. The fossil content and lithology of the Quaternary alluvial plain suggest the deposition of sediments within the littoral zone and estuarine area toward the shallow marine environment of the Holocene Gula Formation. The alluvial deposits consist of silt, sand, clay, gravel, and peat. Seismic reflection surveys in the area suggest that the bedrock depth is well over 200 m (Kamaludin 1990). Personal communication with drillers conversant with geology of the area confirmed that the groundwater is shallow in the region. They explained that during the peak of the rainy season the groundwater depth could be approximately 1 and 2–5 m at other times.

The closed AJL is between two settlements in the outskirts of Seberang Perai (Fig. 1a). The surveyed area at the landfill site lies between latitudes N $5°24'58''$ and N $5°25'14''$ and longitudes E $100°24'13''$ and E $100°24'25''$. This coverage includes most of the 9.3×10^4 m² landfill area. The site, which started as an open dumpsite in 1977, was upgraded to sanitary status in 1999. While in operation, the landfill received approximately 5.9×10^5 kg of municipal and industrial waste per day. The site possesses no base liner, which resulted in heavy pollution of the nearby river and groundwater during the early stages of its operation (Umar et al. 2010). The local authority closed the site in 2001 and later converted it to a transfer station, although it still receives garden waste (Aziz et al. 2012).

The active PBL is within Byram Forest Reserve at Nibong Tebal, Seberang Perai, and a natural marine clay liner overlays the landfill environment (Umar et al. 2010). The landfill, which is on the coast of the Penang Mainland (Fig. 1b), started operation in the 1980s (Muhammad et al. 2008). The PBL is Penang's largest landfill, and it accepts both municipal and industrial solid waste. The surveyed area at the landfill site is within latitudes N $5°12'14.7''$ to N $5°12'22.0''$ and longitudes E $100°25'26.3''$ to E $100°25'38.4''$.

In 1991, the PBL was upgraded to sanitary status level II by a controlled tipping process. The landfill was again enhanced to a sanitary level III in 2001 via implementation of leachate recirculation in addition to the controlled tipping (Aziz et al. 2004). The site comprises of three sections. The survey site was downslope of the landfill toward the leachate channel. This segment, which forms part of the third section, was already overlaid with soil at the time of acquisition. The total area covered by the dumpsite is about 6.2×10^5 m², and it can take in about 1.6×10^6 kg of solid waste daily (Bashir et al. 2010).

A separate landfill, Beriah landfill (BL) at Alor Pongsu, Perak, Malaysia, was selected to assess the chargeability of disseminated leachate. The upgraded semi-aerobic landfill, which is in the same geological setting with landfills

chosen for characterization, is located at latitude N $5°4''$ longitude E $100°35''$. The landfill started as an open dumping site in an area of mainly alluvium deposits consisting of clay, silt, sand, and gravel. According to Bosch (1988), the peat in the Beriah areas overlies the Holocene deposits of the Gula Formation. The unit is also over the Simpang Formation, filling the channel, the depression, and overlying bedrock in some places. The landfill covers an area of about 4.1×10^4 m² of a palm plantation. Since being upgraded in 2000, the site has received approximately 1.8×10^5 kg of domestic waste daily (Syafalni et al. 2014).

Methodology

Data acquisition

The data were acquired from the two sites in December 2012 and January 2013. Rainy season in Peninsular Malaysia peaks during October and November (www.met.gov.my). It is assumed that the precipitation during these months, which is the primary source of any contaminant plumes, would have settled in the host sediments by the time geophysical survey and sampling were conducted.

11 and 10 electrical resistivity/chargeability profiles were acquired in AJL and PBL, respectively, among which only six (Fig. 1a) and five (Fig. 1b) are shown owing to space limitations. Alternate profiles were chosen for display and subsequent interpretation. Figure 1a shows three profiles (400 m) in the SE–NW direction perpendicular to the slope of the landfill, while the other three (200 m) were taken in the NE–SW direction parallel to the slope. Figure 1b shows two lines (400 m) in SE–NW direction and perpendicular to the slope of the landfill and three lines (400 m) conducted SW–NE parallel to the slope of the site. To determine the differences between the subsurface of the contaminated landfills and the uncontaminated surroundings, control lines were carried out upstream of the landfill sites outside the polluted areas.

The 2D resistivity/IP data were acquired simultaneously for each profile using the multi-electrode ABEM Lund Imaging System (Dahlin 1996). The IP acquisition function obtains both resistivity and IP data concurrently. The Lund Imaging System consists of an ABEM TERRAMETER SAS 4000, ES10-64 ELECTRODE SELECTOR, 100 m cable rolls, connectors, and steel electrodes. The selector allows automatic selection of the four active electrodes for each measurement using conventional configurations (Griffiths et al. 1990). The acquisition at both landfills had 50 m intervals between the parallel profiles. The surveys used the Wenner–Schlumberger array with 5 m minimum electrode spacing, n values of 1–6 and a total of 41, and 61

Fig. 1 Maps of landfill sites **a** AJL area showing profiles *A*, *B*, *C*, *D*, *E*, *F*, and the control line **b** PBL site with profiles *G*, *H*, *J*, *K*, *L* and the control line **c** BL area showing assessment lines L1, L2, L3, and the borehole locations BH 1, BH 2, and BH 3
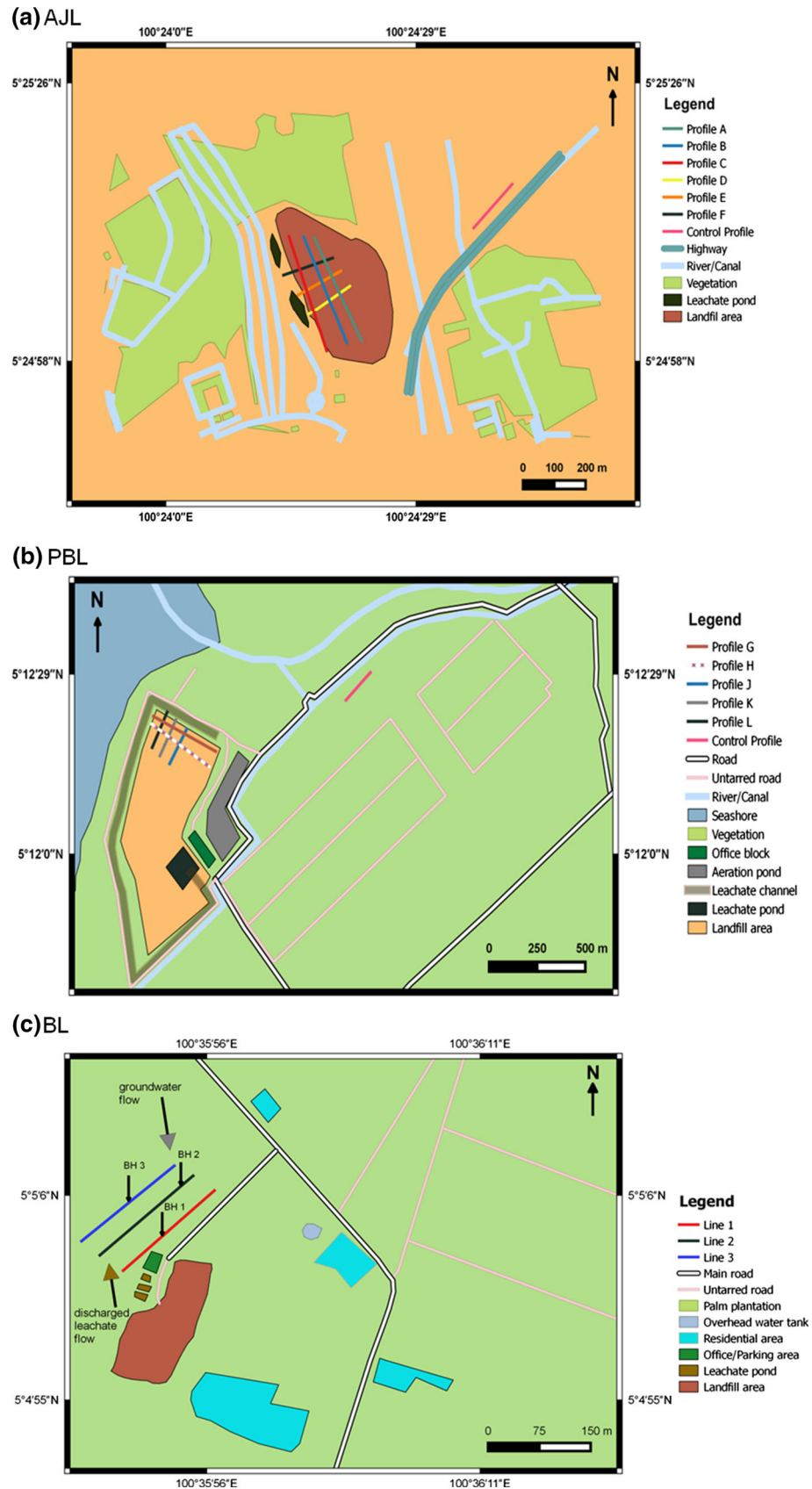
ground insertion points for 200 and 400 m layouts, respectively.

Nonpolarizable electrodes such as lead–lead chloride or copper–copper sulphate electrodes are commonly used in IP acquisition to avoid the charge-up effect usually generated at potential electrodes. Inductive and capacitive coupling of electrical cables produce transient currents in the subsurface that interfere with transmitting signals of the acquisition (Dahlin et al. 2002). However, if the contact resistances between electrodes and ground are minimized, the effects of the coupling can be reduced significantly. In addition, the charge-up effect can be corrected by subtracting the polarization potential measured at the potential electrodes when no primary current and no IP signal are present (Dahlin et al. 2002). Subsequently, the acquisition of good IP data quality using ordinary multicore cables and steel electrodes is possible under these favourable conditions. In situations, in which contact resistance between the electrode and ground is less than 1 kΩ, very high quality IP data can be recorded (Dahlin 2014). Dahlin et al. (2002) investigated two landfill sites in Sweden and compared measurements taken using only stainless steel electrodes with those made using both stainless steel and Pb–PbCl nonpolarizable electrodes employing one or two sets of multicore cables, respectively. They observed insignificant differences between the two datasets, however at one site, the charge-up effect on the potential electrodes was not important while at the other site the correction procedure was essential.

The output current intensity was between 100 and 200 mA for the data acquisition at the landfill sites, while 20–50 mA was used for control lines, which are outside the contaminant zones. The time window of 80–180 ms after current turn-off was used for calculating the chargeability (Dahlin et al. 2002).

To support the interpretation of the inverse models, 11 assessment lines with dipole–dipole configuration were conducted over the surface and diffused leachate at the Beriah Landfill site in January 2013, although only the three with boreholes are shown owing to space limitations (Fig. 1c, lines L1, L2, and L3 run in the SW–NE direction). The plume from aeration ponds discharges downstream into a nearby palm plantation. The 11 evaluation lines are 200 m long and 10 m apart with n values 1–6. However, the three lines shown are about 50 m apart. These lines run over surface leachate along the drainage and a combination of leachate seepages from the drainage and dispersion from the untipped contaminant plumes. This acquisition was used to assess the chargeability response of the dispersed leachate, excluding the influence of solid waste. Soil and leachate/groundwater were sampled from aeration ponds and the three boreholes for physiochemical analysis. To eliminate the direct effects of rainwater and runoff surface water in samples from the boreholes, the in situ content

was flushed out before sampling. The phreatic levels of the wells were also noted before the flushing, after which the recharges were sampled at a depth of 15 m (Table 2).

Data processing

The SAS 4000 Utility software program was used to convert the field data downloaded from ABEM Terrameter SAS 4000 to readable files. The transformed raw resistivity/IP data were later processed using the RES2DINV Geotomo software (www.geotomosoft.com) and Surfer 8 (Golden Software, Colorado, USA). The former was used to invert the resistivity and IP data, while the latter was used to improve visualization of the 2D sections. The resistivity/chargeability values measured are considered as apparent values because they represent a resultant value of the chargeability and resistivity of a subsurface volume. To obtain a true section, an inversion procedure must be applied.

The RES2DINV inversion program employs fast techniques for data inversion developed by Loke and Barker (1996a, b) and Loke et al. (2003). It considers 2D subsurface models composed of rectangular blocks, each one having constant resistivity and chargeability. The distribution and dimensions of the blocks are automatically produced, so that the block number does not surpass the number of measured points. The optimization techniques iteratively minimize the differences between the measured data and the synthetic responses of these models (which are calculated using finite element or finite difference methods), until a final representation of the distribution of resistivity/chargeability in the subsurface is obtained.

The program offers two types of optimization procedures: a common least-squares (L_2-norm) inversion approach (Loke and Barker 1996a, b), and a robust inversion option in which the absolute values (L_1-norm) of data misfit are minimized (Loke et al. 2003). This last procedure is more robust against noise in the data, making it most appropriate for IP data that is sensitive to noise (Dahlin et al. 2010). Regarding model constraints, necessary to stabilize the inversion process, the square or the absolute variations of the resistivity/chargeability values can be minimized. The robust model constraint (L_1-norm) is used for blocky targets, while the standard model constraint (L_2-norm) is used at sites with smooth changes in subsurface properties (Loke et al. 2003). This investigation adopted the L_1-norm, which allows for considerable variation in the inverted models and can address the high electrical resistivity/IP contrasts that are typical of landfills.

The finite difference procedure was selected rather than the finite element for the forward modelling calculations. In view of the significant resistivity and chargeability contrasts expected at the dumpsites, the finest mesh was

Table 1 Inversion parameters and summary of results from inverse models

	Layout length (m)	Acquisition array	Datum points	No. of layers	No. of blocks	Absolute error (%)		No. of iterations
						Resistivity	Chargeability	
Profile A	400	Wenner-Schlumberger	563	13	745	14.5	15.1	4
Profile B	360	Wenner-Schlumberger	459	16	735	11.4	15.6	6
Profile C	400	Wenner-Schlumberger	581	36	1304	12.3	25.4	3
Profile D	200	Wenner-Schlumberger	264	11	283	12.5	18.7	6
Profile E	200	Wenner-Schlumberger	608	20	420	10.6	12.2	3
Profile F	200	Wenner-Schlumberger	621	20	418	14.1	24.2	4
Profile G	400	Wenner-Schlumberger	692	18	899	12.0	10.8	5
Profile H	400	Wenner-Schlumberger	447	17	814	10.9	13.7	5
Profile J	200	Wenner-Schlumberger	202	8	227	14.3	17.8	10
Profile K	200	Wenner-Schlumberger	379	12	302	12.6	14.8	5
Profile L	200	Wenner-Schlumberger	520	18	402	14.5	12.8	4
Line 1	200	Dipole–dipole	349	15	416	15.1	16.2	4
Line 2	200	Dipole–dipole	288	15	407	21.9	17.5	5
Line 3	200	Dipole–dipole	316	9	260	19.2	24.6	4
AJL control profile	200	Wenner-Schlumberger	330	20	408	7.1	3.6	4
PBL control profile	200	Wenner-Schlumberger	282	18	379	26.2	8.6	4

chosen for the forward modelling. Values of 0.05 and 0.005 were selected for the robust data constraint cutoff factor and the robust model constraint cutoff factor, respectively. The initial damping factor for the processing started at 0.16 with a minimum damping factor of 0.03. The IP damping factor selected for the inversion of chargeability data was between 2.5 and 5. The limit range of model resistivity and IP values was 0.02–50 and 0–900, respectively (Ishola et al. 2014). Table 1 contains the inversion parameters adopted for this study, including a summary of the results of the inverse models.

Results and discussion

Beriah landfill (leachate assessment site)

The probable sections in the subsurface of a municipal landfill are the leachate plume, the waste deposits (saturated or unsaturated), and the uncontaminated soil (saturated or unsaturated). In addition, clay, which has a distinct chargeability profile, is used to cover waste intermittently at landfill sites. Among these segments, as mentioned earlier, the interpretation of chargeability anomaly of the disseminated leachate is the most controversial during the analysis of subsurface strata at solid waste disposal sites.

The results of the assessment profiles over the diffused leachate plume exhibited insignificant IP responses from the low resistivity contaminant plumes (Figs. 1c, 2). Table 2 presents physiochemical analyses of leachate/groundwater

samples from the aeration ponds and three boreholes (BH 1, BH 2, and BH 3). Although the leachate plume passed through aeration ponds, significant amounts of pollutants were still subjected to discharge and seepage. In addition, leachate plumes leaking from the untipped plume were noticed disseminating through the base of the landfill. The traces of contaminants were within the aquifers close to the aeration ponds. Higher conductivity was observed in BH 1 (667 $\mu S\ cm^{-1}$) than BH 3 (226 $\mu S\ cm^{-1}$), both of which coincided with a low resistivity leachate zone in the 2D section. However, BH 2 (12 $\mu S\ cm^{-1}$) had the lowest conductivity among the borehole results, confirming that the uncontaminated unit had high resistivity.

Three wells can be used to determine groundwater flow direction in a localized survey area using the trigonometry approach based on the spatial locations of the wells and the phreatic levels. In this method, groundwater heads are used to contour equipotential lines and subsequently flow nets (Domenico and Schwartz 1998). The direction of flow is usually from the higher heads to the lower heads, and perpendicular to the head contour (equipotential) lines in an isotropic media. Consequently, the groundwater/leachate flow direction estimated for the survey area is in the opposite direction to the course of the plume discharged from the aeration ponds (Fig. 1c).

Abu-Zeid et al. (2004) reported that heavy metallic loads exist in the leachate plume as suspended materials, and these insoluble particles promote high IP response through electrode polarization. Conversely, Gallas et al.
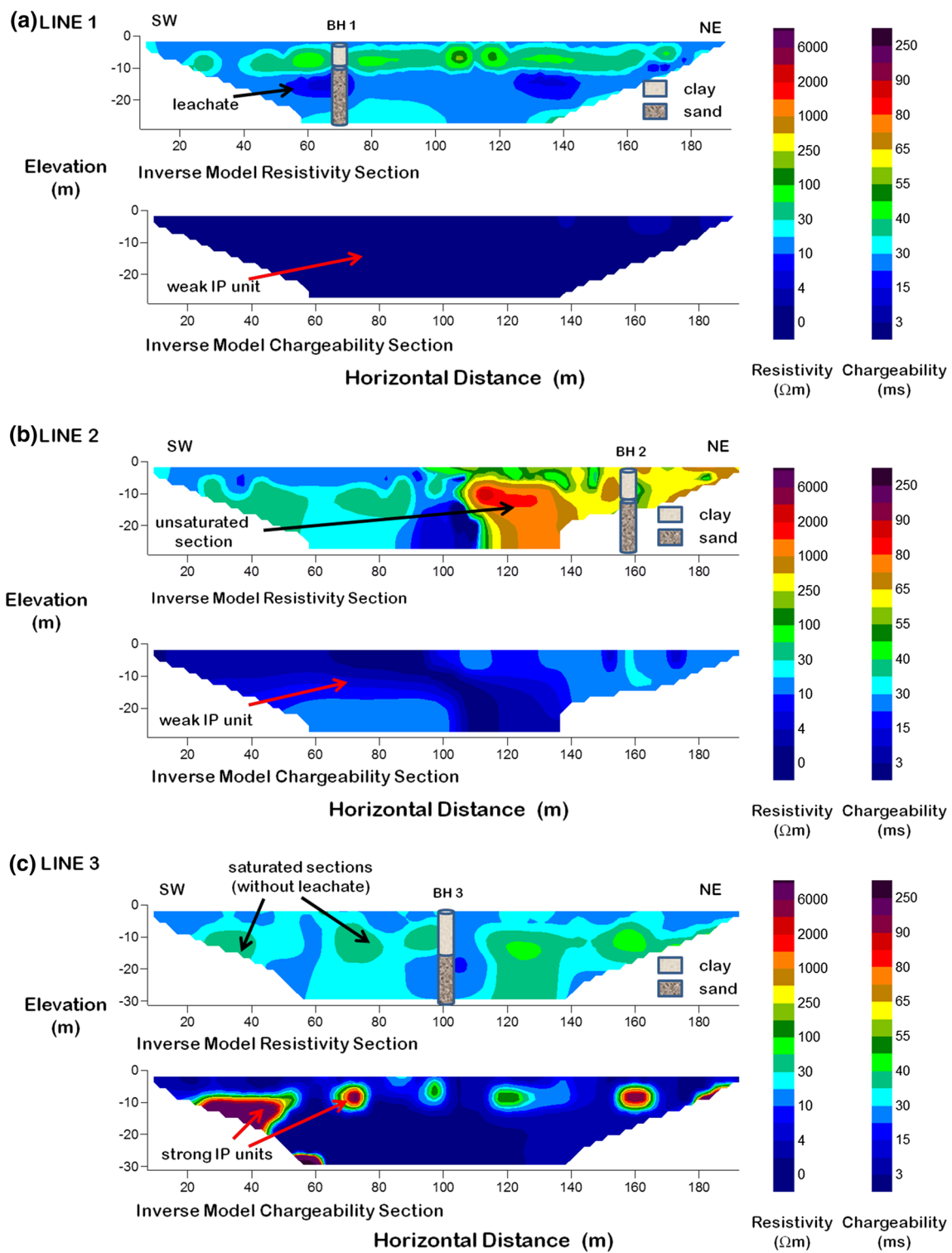
Fig. 2 Electrical resistivity and chargeability inverse models of the assessment lines showing leachate units, IP anomalies, and borehole sections at Beriah Landfill. **a** Line 1; **b** line 2; **c** line 3

(2011) stated that ionic membrane polarization is the only IP response in the leachate, and that this diminishes as ions accumulate. Moreover, they report that the increased ionic concentration reduces the distance of the ionic charges in proximity to the membrane, generating a decrease in IP effects. This impediment in the vicinity of high

Table 2 Analyses of results from leachate/groundwater samples collected from aeration ponds and boreholes at Beriah landfill (leachate assessment site)

Parameter	First aeration pond	Last aeration pond	BH 1	BH 2	BH 3
Phreatic depth	0	0	2	2.5	2.3
Sampling depth	0	0	15	15	15
Clay thickness	Not applicable	Not applicable	10	6	12
Sand thickness	Not applicable	Not applicable	20	24	18
TDS	11,470	6756	4735	78	1514
pH	8.5	8.3	8.3	8.3	8.4
EC	1654	855	667	12	226
BOD	125	86	53	15	27
COD	1243	523	406	243	326
NH_3-N	1325	236	55	2	23
Chloride	722	34	12	6	15
Manganese	3	3	2	0	1
Iron	6	5	4	1	3
Zinc	0.3	0.2	0.2	0	0
Cadmium	0.2	0.1	0.1	0	0.1
Chromium	0.2	0.2	0.1	0	0.1
Nickel	0.3	0.2	0.1	0	0
Lead	3	3	2	0	2
Copper	0.1	0.1	0.1	0	0

All quantities on the table are in mg/L except depth and thickness (in m), pH (in standard units), and EC (in μS/cm)

TDS total dissolved solids, *EC* electrical conductivity, *BOD* biological oxygen demand, *COD* chemical oxygen demand, *NH_3-N* ammoniacal nitrogen

concentrations of ions is due to cation adsorption by clay particles (Schön 1996).

The proportions of heavy metal loads and TDS in disseminated leachate plumes that will produce either electronic or ionic polarization depend on the status of the leachate. The nature and age of solid waste buried, water infiltration rate, pH, and temporal state of biodegradation determine the composition of leachate (Farquhar 1989). The depth of burial of fill, climatic conditions, and variations in the water table, as well as the capping practice and fluid controls influence the quantity of leachate and rate of landfill gas production at landfill sites. The proportion of the metallic loads appears to be lower than the fraction of TDS in disseminated leachate plumes during all leachate biodegradation stages (Meju 2000).

Despite the diminishing membrane polarization with increasing ion accumulation near the membrane in sediments (Gallas et al. 2011), the quantity of TDS is still much greater than that of suspended heavy metals in the disseminated plume samples (Table 2). This proportion established the dominance of membrane polarization over electrode polarization in the plume's IP responses. Thus, the dominant membrane polarization determines the leachate's chargeability status, although the polarization weakens in turn. Accordingly, the results of this study affirm the low chargeability of the diffused leachate plume.

The typical resistivity and chargeability ranges for the different subsurface regions of the landfills were determined based on this assessment and corroboration of the results from inverse models and cited literature (Table 3).

Ampang Jajar landfill

Figures 3 and 4 show six resistivity and chargeability inverse models for the AJL. Figure 3 presents three 400 m models (for Profiles A, B, and C) perpendicular to the slope of the landfill. Figure 4 shows three 200 m models (for Profiles D, E, and F) parallel to the slope of the landfill.

The low resistivity zones (<10 Ωm), which are reflected by blue colour in the inverse models, indicate the leachate plume, which coincides with the shallow localized aquifer. Yoon et al. (2003) and Kaya et al. (2007) interpreted leachate zones to have resistivity values of less than 10 Ωm. As shown by the resistivity models for Profiles A, B, and C, the leachate plume increases downgradient of the landfill (Fig. 3). The growing leachate plume gradually decreases the uncontaminated saturated sections, which are considered intermediate resistivity areas (green colour i.e., 30–150 Ωm). The trend in the plume's variation in the resistivity models confirmed that its mounting tipping load is towards the aeration ponds located downstream of the landfill.

Table 3 Adopted interpretation scheme of the resistivity and chargeability inverse models for the selected landfill sites

Subsurface section	Resistivity	Chargeability
Mixture of leachate and waste	Low (<10 Ωm) (Dahlin et al. 2010)	High (>70 ms) (Dahlin et al. 2010)
Saturated clay (uncontaminated)	Low (<10 Ωm) (Guérin et al. 2004)	High (>70 ms) (Slater et al. 2006; Breede and Kemna 2012; Gazoty et al. 2012b)
Unsaturated waste	High (>1000 Ωm) (Leroux et al. 2007; Dahlin et al. 2010)	High (>70 ms) (Dahlin et al. 2010)
Unsaturated soil	High (>1000 Ωm) (Leroux et al. 2007)	Low (<20 ms) (Leroux et al. 2007)
Leachate Plume	Low (<10 Ωm) (Guérin et al. 2004; Kaya et al. 2007)	Low (<20 ms) (Gallas et al. 2011)
Saturated waste (without leachate)	Intermediate (30–150 Ωm) (Dahlin et al. 2010)	High (>70 ms) (Dahlin et al. 2010)
Saturated soil (uncontaminated)	Intermediate (30–150 Ωm) (Guérin et al. 2004; Dahlin et al. 2010)	Low (<20 ms) (Dahlin et al. 2010)

A sizeable solid waste deposit occupies most of Profile A (Fig. 3a, chargeability model). High chargeability values (>70 ms) within leachate zones (with low resistivity) suggest a mixture of waste and leachate (Dahlin et al. 2010). However, a significant fraction of the large waste body is saturated and without leachate. Waste comprising a considerable fraction of the leachate plume is at the centre of Profile B, as indicated by high chargeability (Fig. 3b) and low resistivity (Fig. 3b). Underneath this waste is a vast unsaturated area characterized by high resistivity (>1000 Ωm) and low chargeability (<20 ms), which implies that the zone is not within the localized aquifer and is also free of waste.

The combination of high chargeability and low resistivity interpreted as waste mixed with leachate could also represent an uncontaminated saturated clayey layer. However, the spread, pattern, and location of the high chargeability zone would distinguish the waste from the clayey sections at a landfill site. The clayey layer, which is usually used as cover material at landfills, displays a thin spread of high chargeability units when saturated and uncontaminated, in contrast with a relatively large waste deposit. Dry clay sections exhibit weak IP effects, similar to other dry unconsolidated sediments. A material with high resistivity and low chargeability can be classified as covering soil material, probably medium grained to coarse-grained (Leroux et al. 2007).

Profile A shows a high resistivity region on the right flank that is correlated with low chargeability. This area is an unsaturated soil free of waste that is probably part of the cover material. Shallow units of high chargeability overlay the medium resistivity zone on the left side of Profile C. These units are considered to be saturated waste without leachate (Fig. 3c). On the other side, a shallow unit of high

chargeability waste spreads from 200 to 300 m, which is within the leachate zones. The accumulated leachate shown on the right flank of the resistivity section of Profile A at about 280 m could serve as a location for an upslope monitoring well (Fig. 3a). The 200 m position on Profile C is most appropriate for a downstream monitoring well, and a borehole drilled at this point to a depth of 40 m could serve as a monitoring well.

The resistivity models of Profiles D, E, and F (Fig. 4) reflect the mounting leachate plume, similar to the preceding perpendicular profiles (Fig. 3). In this case, the rising plume load is not parallel to the landfill gradient, and the flow may respond to an alternative tipping or underground preferential flow. Surface cover material is displayed by inverted sections of Profile D, which was confirmed by the high resistivity and low chargeability. This dry clayey cover without vegetation stretches from about 70 m to the right end of the profile (Fig. 4a).

Profile D contains two anomalies with high IP responses considered waste sections. The larger waste deposit, which is on the right side of the chargeability model, has minimal leachate, and is thus mostly outside the leachate zones. However, the small unit on the left flank is within the leachate areas. Profile E also shows two isolated waste deposits immersed in the accumulated contaminant plume (Fig. 4b). In view of their corresponding locations, the identified deposits appear to be extensions of the waste units previously detected in Profile D. In contrast with the dry surface of Profile D, Profiles E and F have saturated soil covers. The inverted models for Profile F are on a buffer zone free of waste, and the region serves as a passage for diffused leachate en route to the collection ponds (Fig. 4c).
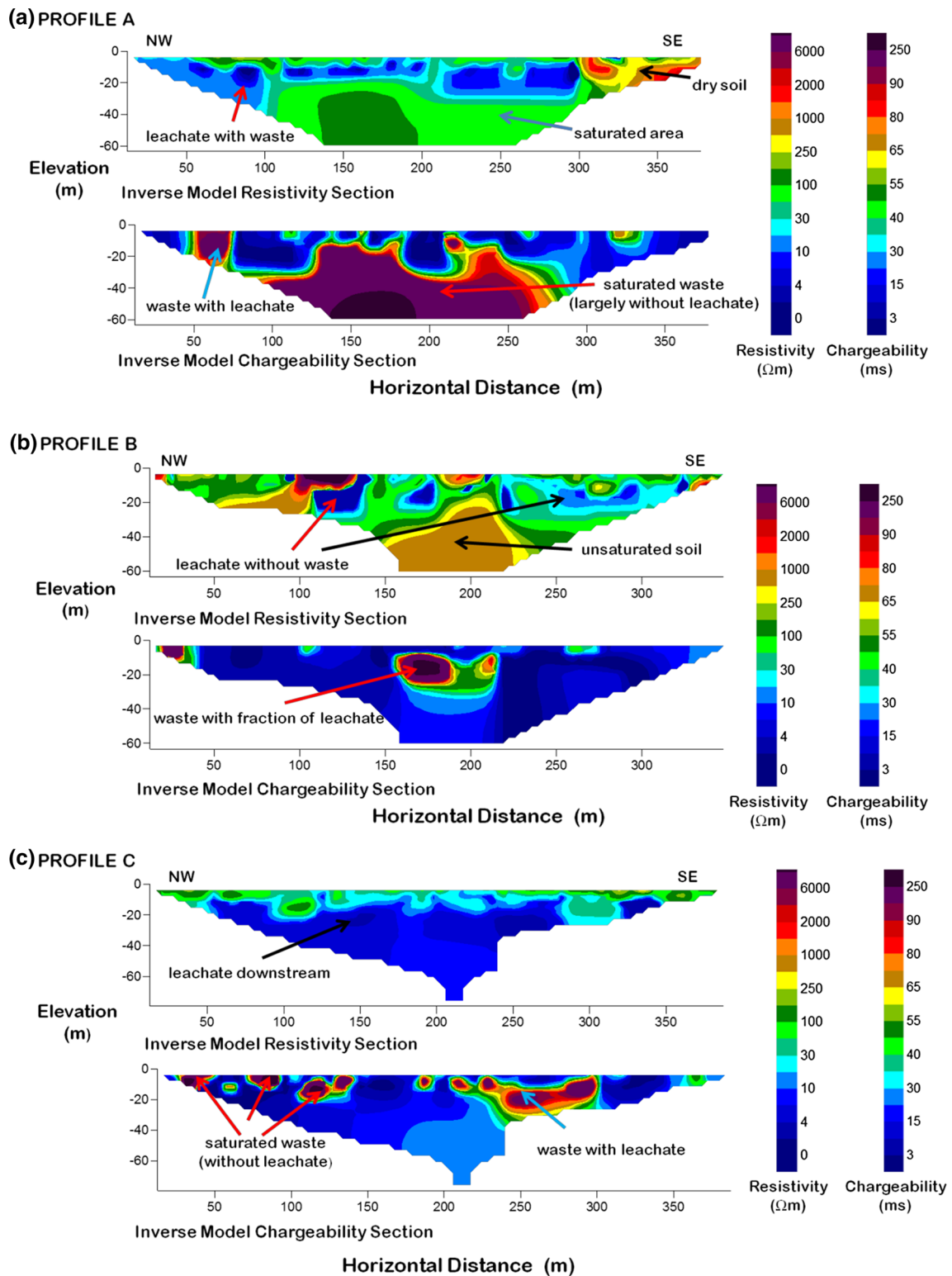
Fig. 3 Electrical resistivity and chargeability inverse models of profiles perpendicular to the slope of AJL depicting different strata beneath the landfill. a Profile A; b profile B; c profile C
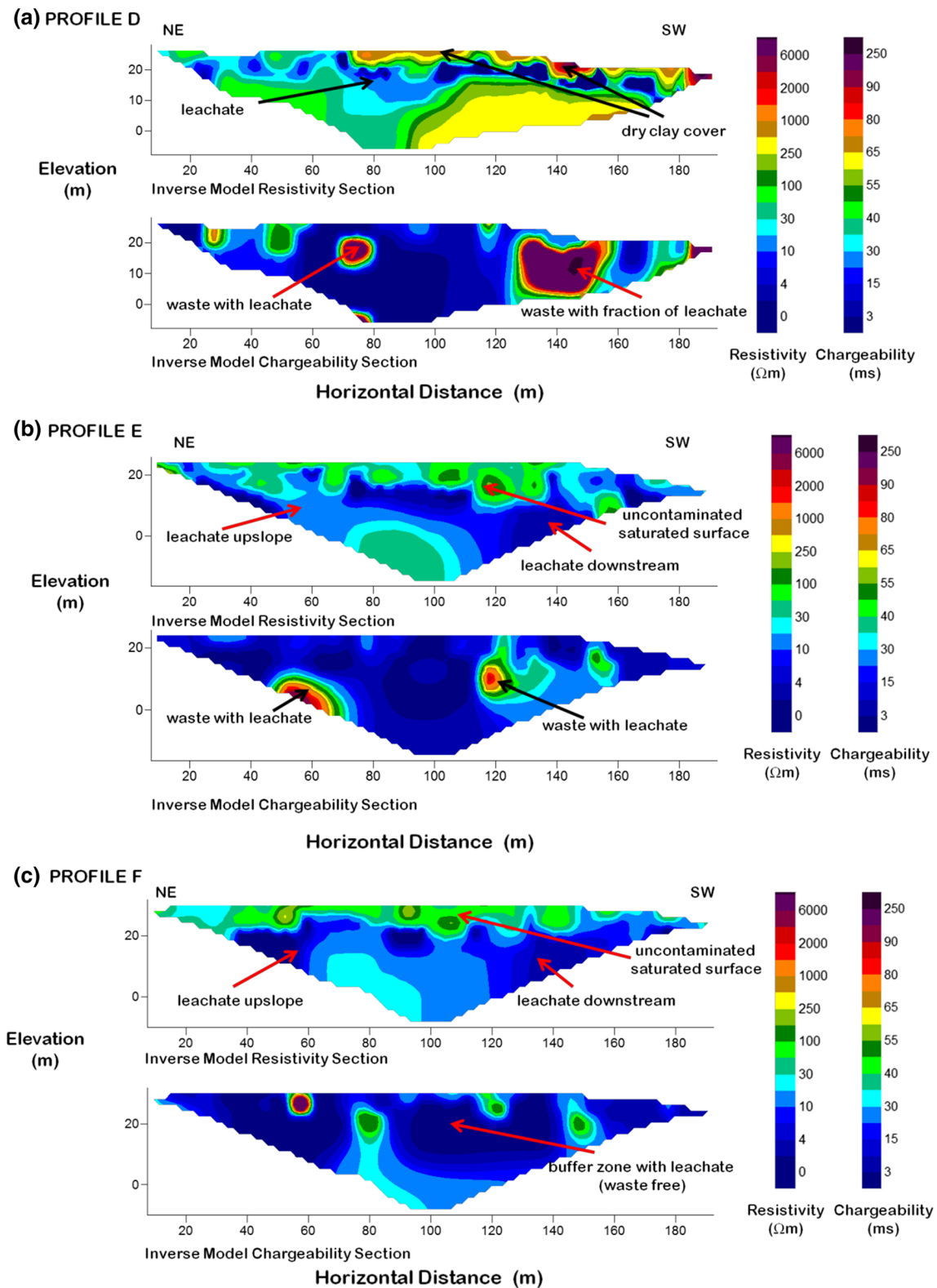
Fig. 4 Resistivity and chargeability models of profiles parallel to the slope of AJL distinguishing the strata beneath the landfill. **a** Profile D; **b** profile E; **c** profile F

Pulau Burung landfill

Figures 5 and 6 show five of the ten inverted models for PBL. Figure 5 displays two 400 m inverted models (for Profiles G and H), which are perpendicular to the slope of the landfill. Figure 6 has three 200 m imaged sections (for Profiles J, K, and L) parallel to the slope of the site. The resistivity models shown in Figs. 5 and 6 depict identical massive dispersion of leachate, regardless of the distance of each profile to the aeration channel. The high resistivity spread on the surface from 65 to 180 m on Profile G suggests an unsaturated soil, which is probably part of the clay cover material (Fig. 5a). The unsaturated units extend to a depth of about 20 m, with unsaturated waste deposits evident within these units based on the high chargeability and corresponding high resistivity.

Profile G has a large waste deposit at its centre. To the right of this waste are minute high IP responses at shallow depths (Fig. 5a). The near surface spread of these high chargeability units suggests that they are likely to be part of the saturated and uncontaminated clayey cover. The inverse models of Profile H present a surface with intermediate resistivity and low chargeability (Fig. 5b), which signifies a saturated, but uncontaminated soil. The right end of the models shows an exposed dry waste to a depth of about 20 m, which was confirmed by high chargeability and resistivity values. Two isolated saturated waste deposits, possibly extensions of the massive waste observed in Profile G, are located at 120 and 170 m in the chargeability model of Profile H (Fig. 5b). These deposits are without leachate, manifested by the intermediate resistivity values. However, a waste deposit saturated with
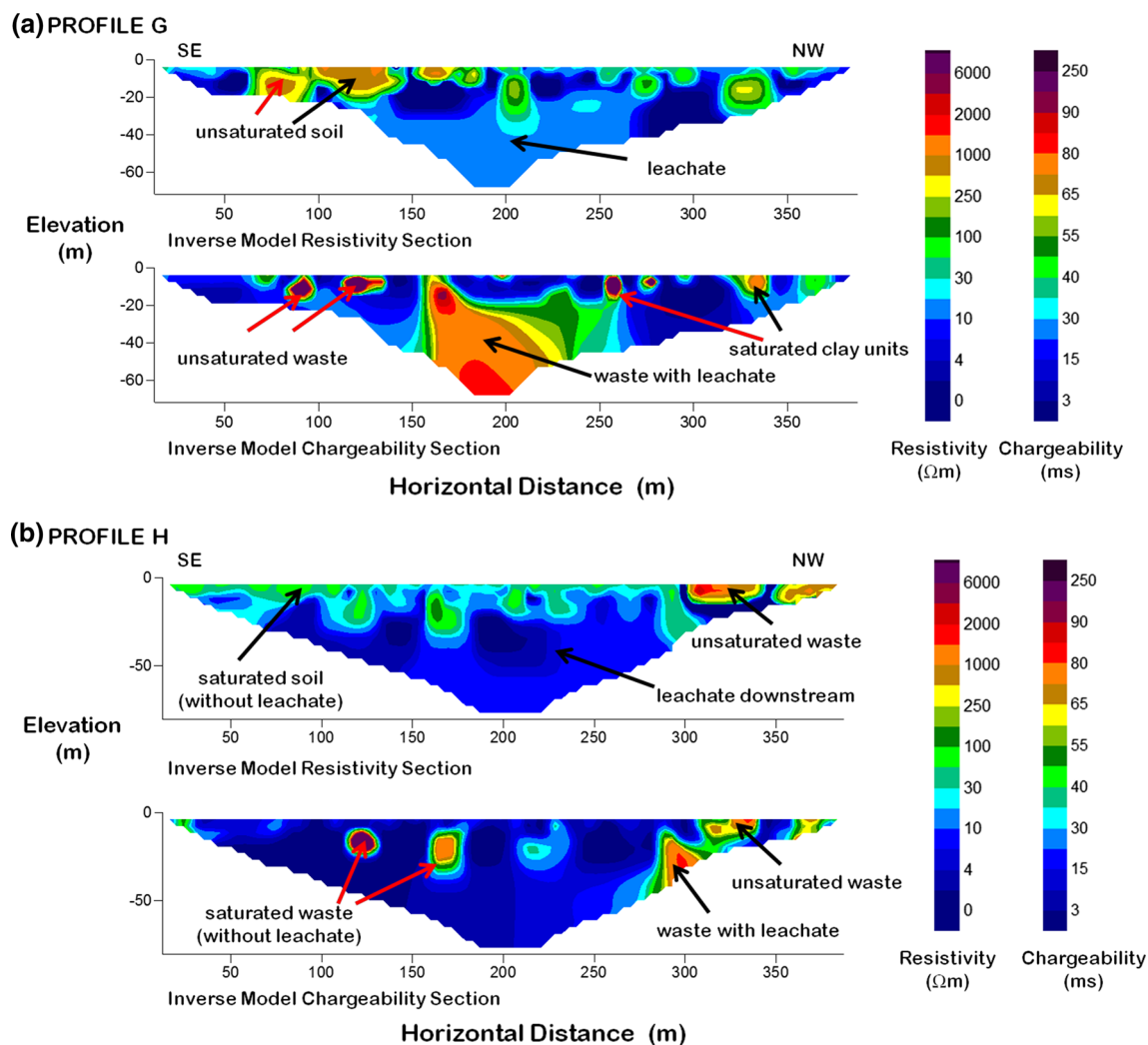

Fig. 5 Resistivity and chargeability inverse models of profiles perpendicular to the gradient of PBL, differentiating the landfill's subsurface. a Profile G; b profile H
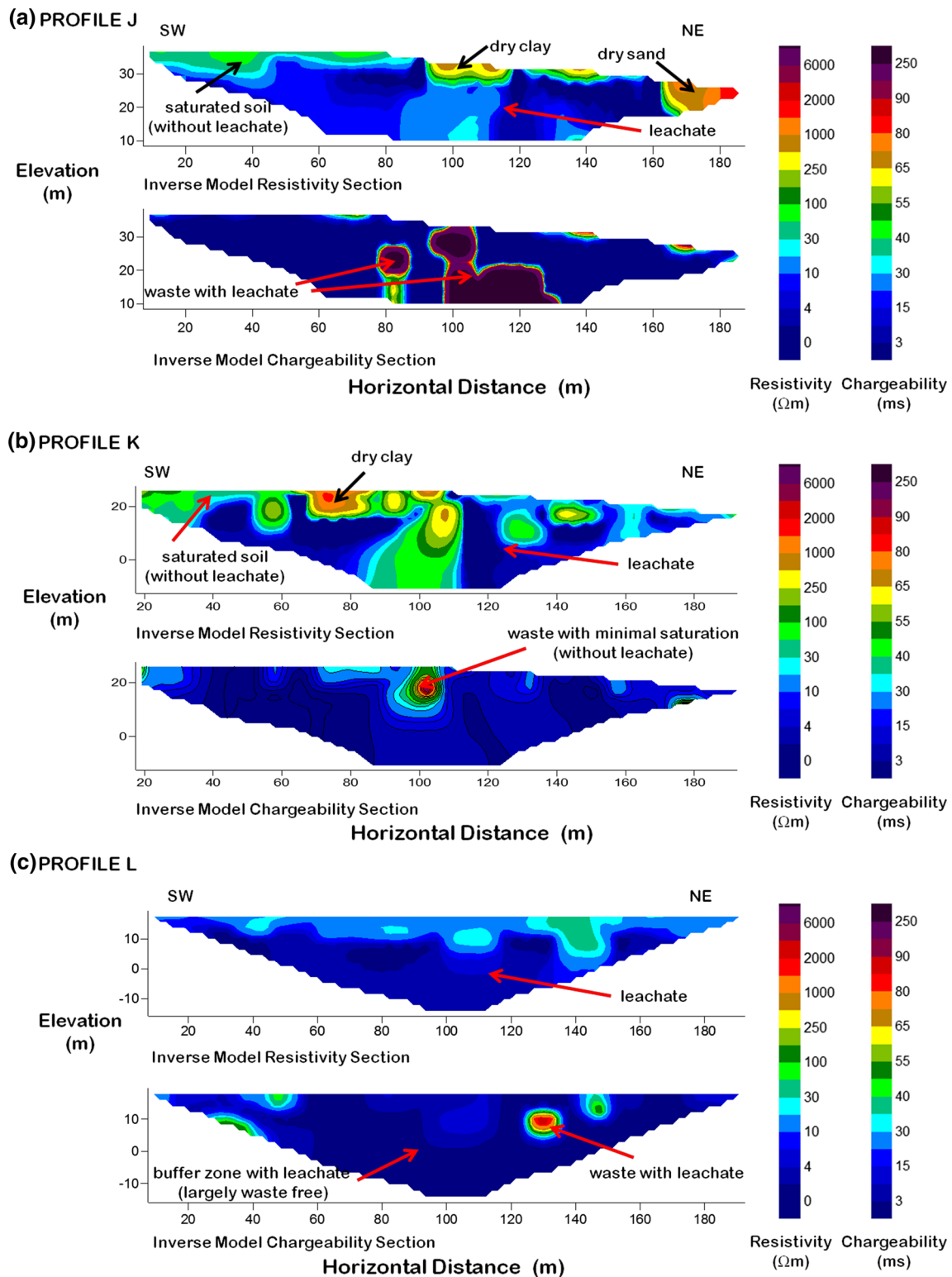
Fig. 6 Resistivity and chargeability inverse models of profiles parallel to the gradient of PBL showing the classification of strata underneath the landfill. **a** Profile J; **b** profile K; **c** profile L
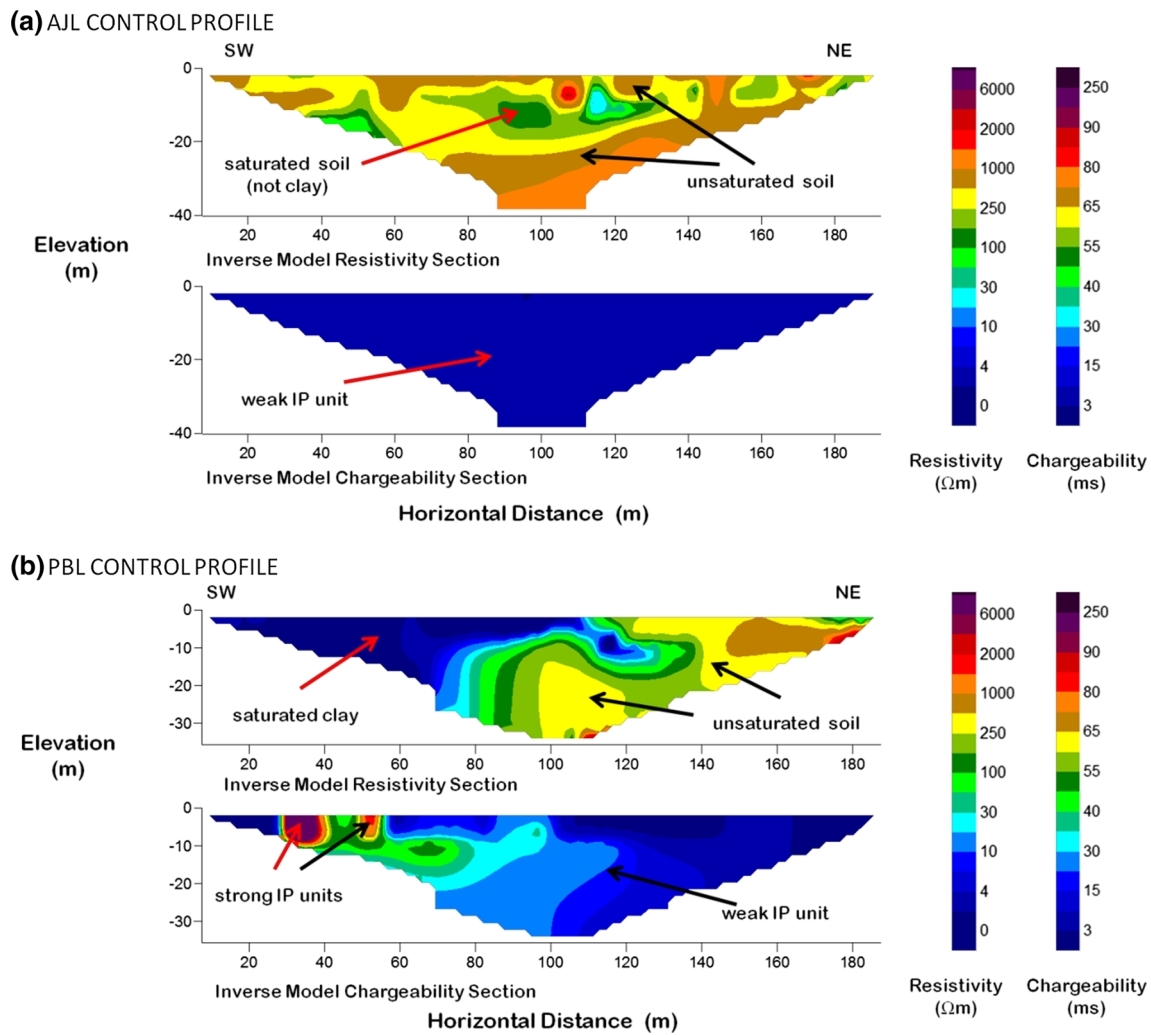
Fig. 7 Resistivity and chargeability inverse models of the control profiles. a AJL; b PBL

leachate is present at almost the same depth coinciding with 300 m.

Resistivity models for Profiles J, K, and L display the massive build-up of leachate discharging to the aeration channel (Fig. 6), although part of the source of this accumulated plume could be from other sections of the landfill (Fig. 1b). The central part of Profile J shows a considerable amount of solid waste submerged in leachate, while Profiles K and L show an insignificant quantity of waste deposits (Fig. 6). Uncontaminated saturated soil covers the surface of Profile J from 0–90 m, while 90–145 m is dry land, which is most likely the clay cap (Fig. 6a). Exposed units of unsaturated soil confirmed to be sand, based on surface observations lie at the end of the profile.

Most of the surface of Profile K (Fig. 6b) is uncontaminated saturated soil (intermediate resistivity and low chargeability), with a few areas that are dry land (high resistivity and low chargeability). Figure 6c presents

Profile L, which consisted of a leachate plume mostly free of waste deposits and considered to be within the buffer zone between the waste deposits and the leachate channel. The chargeability models of Profiles K and L show isolated waste deposits of similar extent. A fraction of the waste deposits in Profile K are saturated without leachate, while those in Profile L are completely in the contaminant plume.

Based on the accrued leachate plume, the 160 and 280 m marks on Profile G are ideal points for upslope monitoring wells (Fig. 5a). The downstream well could be at the 200 m mark on Profile H (Fig. 5b). Based on the plume spreads, the surveyed area of this active landfill contains fewer waste deposits and greater amounts of leachate plume than the closed AJL.

Additional information from the control profiles shows the contrast in resistivity and chargeability between surveyed landfill sites and uncontaminated areas (Fig. 7). The responses from uncontaminated saturated clay zones

are similar to the signals of waste deposits. Nevertheless, the nonchargeable nature of the leachate plume postulated in this study differentiates the contaminant from saturated clayey sections outside the landfill waste boundaries.

Conclusions

Integration of the electrical resistivity and the time domain IP methods clearly allowed differentiating waste deposits from the leachate plumes and confirmed the regions of the mixture of the two sections. The low resistivity and high IP responses in the orthogonal profiles aided determination of the direction of leachate flow and detection of the waste boundaries. Analysis of the inverted models obtained at the active and closed landfills established the differences in the spread of the contaminant plumes between the two sites. A plan for monitoring, remediation, or reclamation of landfills should include size or quality of waste, quantity of leachate and potential locations for monitoring wells and plume leakages. A full characterization of the landfill's subsurface provides a platform for its management strategies.

The inverse models from the two selected landfills and the assessment lines showed comparable trends in resistivity and chargeability distribution, which is in accordance with the results of previous studies. In addition, this study adopted an analysis chart for the interpretation of resistivity and chargeability models during characterization of the subsurface of the selected landfills. This scheme assigns low (<10 Ωm), intermediate (30–150 Ωm), and high (>1000 Ωm) resistivities. The IP responses have low (<20 ms) and high (>70 ms) chargeability values, while the values absent from the chart are considered transition zones between neighbouring strata.

The assessment of the chargeability status of the wastefree leachate plume attempts to address one of the main challenges of IP surveys at solid waste dumpsites. However, the application of the interpretation scheme is limited in the similarity displayed by resistivity and chargeability values of the uncontaminated saturated clay and the waste mixed with leachate. Furthermore, the layouts limit the depth to which possible contaminant leakages can be investigated. A 3D survey with a lower separation between the profiles would provide an enhanced image of the subsurface, but this would be more expensive and time consuming. The landfill sites selected for this study are all within the unconsolidated sediments; therefore, future investigations are needed to enable application of this characterization procedure to landfills on the consolidated basement.

References

Abdulrahman A, Nawawi MNM, Saad R, Adiat KAN (2013) Volumetric assessment of leachate from solid waste using 2D and 3D electrical resistivity imaging. Adv Mater Res 726: 3014–3022. doi:10.4028/www.scientific.net/AMR.726-731.3014

Abu-Zeid N, Bianchini G, Santarato G, Vaccaro C (2004) Geochemical characterisation and geophysical mapping of landfill leachates: the Marozzo canal case study (NE Italy). Environ Geol 45(4):439–447. doi:10.1007/s00254-003-0895-x

Aluko OO, Sridhar M (2005) Application of constructed wetlands to the treatment of leachates from a municipal solid waste landfill in Ibadan, Nigeria. J Environ Health 67(10):58–62

Archie GE (1942) The electrical resistivity log as an aid in determining some reservoir characteristics. Trans AIMe 146(99):54–62

Aristodemou E, Thomas-Betts A (2000) DC resistivity and induced polarisation investigations at a waste disposal site and its environments. J Appl Geophys 44(2):275–302. doi:10.1016/S0926-9851(99)00022-1

Aziz HA, Adlan MN, Amilin K, Yusoff MS, Ramly NH, Umar M (2012) Quantification of leachate generation rate from a semi-aerobic landfill in Malaysia. Environ Eng Manage J 11(9): 1581–1585

Aziz HA, Yusoff MS, Adlan MN, Adnan NH, Alias S (2004) Physico-chemical removal of iron from semi-aerobic landfill leachate by limestone filter. Waste Manage 24(4):353–358. doi:10.1016/j.wasman.2003.10.006

Bashir MJ, Aziz HA, Yusoff MS, Aziz SQ, Mohajeri S (2010) Stabilized sanitary landfill leachate treatment using anionic resin: treatment optimization by response surface methodology. J Hazard Mater 182(1):115–122

Bernstone C, Dahlin T (1999) Assessment of two automated electrical resistivity data acquisition systems for landfill location surveys: two case studies. J Environ Eng Geophys 4(2):113–121. doi:10.4133/JEEG4.2.113

Bosch JHA (1988) The Quaternary Deposits in the Coastal Plains of Peninsular Malaysia Geological Survey Malaysia. Report No. QG/1 of 1988

Breede K, Kemna A (2012) Spectral induced polarization measurements on variably saturated sand-clay mixtures. Near Surf Geophys 10(6):479–489. doi:10.3997/1873-0604.2012048

Carlson NR, Hare JL, Zonge KL (2001) Buried landfill delineation with induced polarization: progress and problems. Paper presented at the Proceedings 14th meeting Symposium on the Application of Geophysics to Engineering and Environmental Problems (SAGEEP), Denver

Chambers JE, Kuras O, Meldrum PI, Ogilvy RD, Hollands J (2006) Electrical resistivity tomography applied to geologic, hydrogeologic, and engineering investigations at a former waste-disposal site. Geophysics 71(6):B231–B239. doi:10.1190/1.2360184

Dahlin T (1996) 2D Resistivity surveying for environmental and engineering applications. First Break. doi:10.3997/1365-2397.1996014

Dahlin T (2014) Factors affecting time domain IP quality. 3rd International Workshop on Induced Polarization. Oléron Island, France

Dahlin T, Leroux V, Nissen J (2002) Measuring techniques in induced polarisation imaging. J Appl Geophys 50(3):279–298. doi:10.1016/S0926-9851(02)00148-9

Dahlin T, Rosqvist H, Leroux V (2010) Resistivity-IP for landfill applications. First Break 28(8):101–105 (id: 2344519)

Domenico PA, Schwartz FW (1998) Physical and chemical hydrogeology, 2nd edn. John Wiley and Sons Inc, New York

Farquhar G (1989) Leachate: production and characterization. Can J Civ Eng 16(3):317–325. doi:10.1139/l89-057

Frohlich RK, Urish DW, Fuller J, O'Reilly M (1994) Use of geoelectrical methods in groundwater pollution surveys in a coastal environment. J Appl Geophys 32(2):139–154. doi:10.1016/0926-9851(94)90016-7

Gallas JDF, Taioli F, Malagutti Filho W (2011) Induced polarization, resistivity, and self-potential: a case history of contamination evaluation due to landfill leakage. Environ Earth Sci 63(2):251–261. doi:10.1007/s12665-010-0696-y

Gazoty A, Fiandaca G, Pedersen J, Auken E, Christiansen A (2012a) Mapping landfills with Time Domain IP: the Eskelund case study. Near Surf Geophys 10:563–574. doi:10.3997/1873-0604.2012046

Gazoty A, Fiandaca G, Pedersen J, Auken E, Christiansen A, Pedersen J (2012b) Application of time-domain induced polarization to the mapping of lithotypes in a landfill site. Hydrol Earth Syst Sci 16(6):1793–1804. doi:10.5194/hess-16-1793-2012

Griffiths D, Turnbull J, Olayinka A (1990) Two-dimensional resistivity mapping with a computer-controlled array. First Break. doi:10.3997/1365-2397.1990008

Guérin R, Munoz ML, Aran C, Laperrelle C, Hidra M, Drouart E, Grellier S (2004) Leachate recirculation: moisture content assessment by means of a geophysical technique. Waste Manage 24(8):785–794. doi:10.1016/j.wasman.2004.03.010

Iliceto V, Santarato G, Veronese S (1982) An approach to the identification of fine sediments by induced polarization laboratory measurements. Geophys Prospect 30(3):331–347. doi:10.1111/j.1365-2478.1982.tb01310.x

Inanc B, Idris A, Terazono A, Sakai SI (2004) Development of a database of landfills and dump sites in Asian countries. J Mater Cycles Waste Manage 6(2):97–103. doi:10.1007/s10163-004-0116-z

Ishola KS, Nawawi MNM, Abdullah K (2014) Combining multiple electrode arrays for two-dimensional electrical resistivity imaging using the unsupervised classification technique. Pure Appl Geophys. doi:10.1007/s00024-014-1007-4

Kamaludin B (1990) A summary of the quaternary geology investigations in Seberang Perai, Pulau Pinang, and Kuala Kurau. Geol Soc Malaysia Bull 26:47–54

Kaya MA, Özürlan G, Şengül E (2007) Delineation of soil and groundwater contamination using geophysical methods at a waste disposal site in Çanakkale, Turkey. Environ Monit Assess 135(1–3):441–446. doi:10.1007/s10661-007-9662-x

Kelly WE (1976) Geoelectric sounding for delineating ground-water contamination. Groundwater 14(1):6–10. doi:10.1111/j.1745-6584.1976.tb03626.x

Legaz A, Christiansen AV, Auken E, Pedersen J, Fiandaca G (2010) Evaluation of landfill disposal boundaries by means of induced polarization and electrical resistivity imaging. Nordrocs, Copenhagen

Leroux V, Dahlin T, Svensson M (2007) Dense resistivity and induced polarization profiling for a landfill restoration project at Härlöv. Southern Sweden. Waste Manage Res 25(1):49–60. doi:10.1177/0734242X07073668

Loke MH, Acworth I, Dahlin T (2003) A comparison of smooth and blocky inversion methods in 2D electrical imaging surveys. Explor Geophys 34(3):182–187. doi:10.1071/EG03182

Loke MH, Barker RD (1996a) Rapid least-squares inversion of apparent resistivity pseudosections by a quasi-Newton method. Geophys Prospect 44(1):131–152. doi:10.1111/j.1365-2478.1996.tb00142.x

Loke MH, Barker RD (1996b) Practical techniques for 3D resistivity surveys and data inversion. Geophys Prospect 44(3):499–523. doi:10.1111/j.1365-2478.1996.tb00162.x

Martinho E, Almeida F (2006) 3D behaviour of contamination in landfill sites using 2D resistivity/IP imaging: case studies in Portugal. Environ Geol 49(7):1071–1078. doi:10.1007/s00254-005-0151-7

Meju MA (2000) Geoelectrical investigation of old/abandoned, covered landfill sites in urban areas: model development with a genetic diagnosis approach. J Appl Geophys 44(2):115–150. doi:10.1016/S0926-9851(00)00011-2

Morris JW, Barlaz MA (2011) A performance-based system for the long-term management of municipal waste landfills. Waste Manage 31(4):649–662. doi:10.1016/j.wasman.2010.11.018

Mota R, Monteiro Santos F, Mateus A, Marques F, Gonçalves M, Figueiras J, Amaral H (2004) Granite fracturing and incipient pollution beneath a recent landfill facility as detected by geoelectrical surveys. J Appl Geophys 57(1):11–22. doi:10.1016/j.jappgeo.2004.08.007

Muhammad NS, Hambali S, Romali NHM, Shani NM (2008) The effectiveness of leachate treatment in Pulau Burung sanitary landfill, Pulau Pinang. ESTEEM 4:35–44

Naudet V, Revil A, Rizzo E, Bottero JY, Bégassat P (2004) Groundwater redox conditions and conductivity in a contaminant plume from geoelectrical investigations. Hydrol Earth Syst Sci Discuss 8(1):8–22 (HAL Id: hal-00330848)

Schön JH (1996) Physical properties of rocks—fundamentals and principles of petrophysics. Pergamon Press, Oxford, p 583

Sharma PV (1997) Environmental and engineering geophysics. Cambridge University Press, Cambridge

Singh RP, Singh P, Araujo ASF, Ibrahim MH, Sulaiman O (2011) Management of urban solid waste: vermicomposting a sustainable option. Resour Conserv Recycl 55(7):719–729. doi:10.1016/j.resconrec.2011.02.005

Slater LD, Lesmes D (2002) IP interpretation in environmental investigations. Geophysics 1:77–88. doi:10.1190/1.1451353

Slater L, Ntarlagiannis D, Wishart D (2006) On the relationship between induced polarization and surface area in metal-sand and clay-sand mixtures. Geophysics 71(2):A1–A5. doi:10.1190/1.2187707

Soupios P, Papadopoulos N, Papadopoulos I, Kouli M, Vallianatos F, Sarris A, Manios T (2007) Application of integrated methods in mapping waste disposal areas. Environ Geol 53(3):661–675. doi:10.1007/s00254-007-0681-2

Syafalni S, Zawawi MH, Abustan I (2014) Isotopic and hydrochemistry fingerprinting of leachate migration in shallow groundwater at controlled and uncontrolled landfill sites. World Appl Sci J 31(6):1198–1206. doi:10.5829/idosi.wasj.2014.31.06.217

Turesson A, Lind G (2005) Evaluation of electrical methods, seismic refraction and ground-penetrating radar to identify clays below sands—two case studies in SW Sweden. Near Surf Geophys 3(2):59–70. doi:10.3997/1873-0604.2005001

Umar M, Aziz HA, Yusoff MS (2010) Variability of parameters involved in leachate pollution index and determination of LPI from four landfills in Malaysia. Int J Chem Eng. doi:10.1155/2010/747953

Ustra AT, Elis VR, Mondelli G, Zuquette LV, Giacheti HL (2012) Case study: a 3D resistivity and induced polarization imaging from downstream a waste disposal site in Brazil. Environ Earth Sci 66(3):763–772. doi:10.1007/s12665-011-1284-5

Wynn J, Grosz A (2000) Induced polarization—a tool for mapping titanium-bearing placers, hidden metallic objects, and urban waste on and beneath the seafloor. J Environ Eng Geophys 5(3):27–35. doi:10.4133/JEEG5.3.27

Yoon J, Lee K, Kwon B, Han W (2003) Geoelectrical surveys of the Nanjido waste landfill in Seoul, Korea. Environ Geol 43(6):654–666. doi:10.1007/s00254-002-0670-4